

Identification of cooperative genes for *NUP98-HOXA9* in myeloid leukemogenesis using a mouse model

Masayuki Iwasaki, Takeshi Kuwata, Yukari Yamazaki, Nancy A. Jenkins, Neal G. Copeland, Motomi Osato, Yoshiaki Ito, Evert Kroon, Guy Sauvageau, and Takuro Nakamura

The chromosomal translocation t(7;11)(p15;p15), observed in human myeloid leukemia, results in a *NUP98* and *HOXA9* gene fusion. We generated a transgenic mouse line that specifically expressed the chimeric *NUP98-HOXA9* gene in the myeloid lineage. While only 20% of the transgenic mice progressed to leukemia after a latency period, myeloid progenitor cells from nonleukemic transgenic mice still exhibited increased proliferative potential. This suggested that the *NUP98-*

***HOXA9* fusion induced a preleukemic phase, and other factors were required for complete leukemogenesis. *NUP98-HOXA9* expression promoted the onset of retrovirus-induced BXH2 myeloid leukemia. This phenomenon was used to identify cooperative disease genes as common integration sites (CISs). *Meis1*, a known *HOX* cofactor, was identified as a CIS with a higher integration frequency in transgenic than in wild-type BXH2 mice. By the same means we identified further 4**

candidate cooperative genes, *Dnalc4*, *Fcgr2b*, *Fcrl*, and *Con1*. These genes cooperated with *NUP98-HOXA9* in transforming NIH 3T3 cells. The system described here is a powerful tool to identify cooperative oncogenes and will assist in the clarification of the multistep process of carcinogenesis. (Blood. 2005;105:784-793)

© 2005 by The American Society of Hematology

Introduction

Carcinogenesis requires mutations in multiple genetic loci, and many genes involved in regulation of the cell cycle, apoptosis, transcription, and signaling have been identified as critical disease genes.¹ Previous studies have found that combinations of genetic abnormalities are required to make normal cells become cancer cells *in vitro*.² However, it remains unclear how individual genetic mutations cooperate with each other in human cancer. Retroviral insertional mutagenesis is a powerful technique to isolate causative disease genes, and a variety of important genes have already been identified using this method.³⁻⁵ Studies have applied this technique to the identification of oncogenes that collaborate with cell cycle regulators, such as *Cdkn2a* and *p27^{Kip1}*.^{6,7} Therefore, the combination of retroviral insertional mutagenesis and an appropriate animal model with a phenotype similar to that of a human cancer should provide an ideal experimental system to identify cooperative cancer genes. These genes are extremely important, as they could be used to prevent the cancer progression of premalignant lesions or neoplasms with low malignant potential that contain known primary genetic events.

Chromosomal translocations and genetic chimerism in human hematopoietic and soft tissue neoplasms are early genetic events. However, several reports have indicated that chromosomal translocation and chimeric protein expression alone are insuffi-

cient for complete carcinogenesis.⁸ Therefore, it is of great interest to discover which genes cooperate with chimeric oncogenes in carcinogenesis and to what genetic pathways these cooperative oncogenes belong.

The nucleoporin gene *NUP98* on human chromosome 11p15 is involved in a series of relatively rare but recurrent translocations observed in *de novo* acute and chronic myeloid leukemias, as well as in therapy-related myelodysplastic syndrome (t-MDS) and acute myeloid leukemia (t-AML). The major targets of *NUP98* as fusion partners are clustered and nonclustered homeobox genes, including *HOXA9*,^{9,10} *HOXA11*, *HOXA13*,¹¹ *HOXC11*,¹² *HOXC13*,¹³ *HOXD11*,¹⁴ *HOXD13*,¹⁵ and *PMX1*.¹⁶ *HOXA9* is the most frequent fusion partner of *NUP98* in chromosomal translocations.¹⁷ The *NUP98-HOXA9* oncoprotein retains the homeodomain of *HOXA9* and the phenylalanine-glycine (FG) repeat region of *NUP98*.^{9,10} Enforced expression of *NUP98-HOXA9* in NIH 3T3 cells results in transformation. The oncogenic potential of *NUP98-HOXA9* is thought to involve the FG repeats, which are capable of interacting with the transcriptional co-activator, CREB (cyclic adenosine monophosphate response element binding protein) binding protein (CBP)/p300.¹⁸

The leukemogenic potential of murine *Hoxa9* was directly assessed in hemopoietic chimeras where its overexpression in bone

From the Department of Carcinogenesis, The Cancer Institute, Japanese Foundation for Cancer Research, Tokyo, Japan; the Mouse Cancer Genetics Program, National Cancer Institute, Frederick Cancer Research and Development Center, Frederick, MD; the Institute of Molecular and Cell Biology and Oncology Research Institute, Singapore, Singapore; and the Laboratory of Molecular Genetics of Hemopoietic Stem Cells, Clinical Research Institute of Montreal, Montreal, Quebec, Canada.

Submitted April 20, 2004; accepted August 29, 2004. Prepublished online as *Blood* First Edition Paper, September 28, 2004; DOI 10.1182/blood-2004-04-1508.

Supported in part by a Grant-in-Aid for Scientific Research on Priority Areas from the Ministry of Education, Culture, Sports, Science and Technology,

Japan; and by the National Cancer Institute (NCI), Department of Health and Human Services.

The online version of the article contains a data supplement.

Reprints: Takuro Nakamura, Department of Carcinogenesis, Japanese Foundation for Cancer Research, 1-37-1 Kami-Ikebukuro, Toshima-ku, Tokyo 170-8455, Japan; e-mail: takuro-ind@umin.ac.jp.

The publication costs of this article were defrayed in part by page charge payment. Therefore, and solely to indicate this fact, this article is hereby marked "advertisement" in accordance with 18 U.S.C. section 1734.

© 2005 by The American Society of Hematology

marrow cells induced AML after a latency period.¹⁹ In addition, *Meis1*, together with *Hoxa7* or *Hoxa9*, was a frequent target of endogenous retroviral insertional activation in BXH2 mouse leukemic cells, which suggested leukemogenic cooperation between *Meis1* and the *Hox* genes.²⁰ In support of this hypothesis, *Meis1* coexpression dramatically reduced the latency period of *Hoxa9*-induced AML.¹⁹ Also, the trimeric DNA binding complex consisting of *Hoxa9* and MEINOX family homeoproteins such as Meis and PBX was observed in leukemic cells, *Hoxa9* transcriptional activity requires Meis and PBX interaction domains. *Meis1* also cooperated with *HOXB3*, a homeobox gene functionally divergent from *HOXA9*, which suggested that Meis1 might be a common leukemogenic collaborator.²¹ However, as in vitro immortalization of myeloid progenitor cells by *Hoxa9* was reported to occur in the absence of *Meis* expression and *Hoxa9*-PBX interaction,²² a subset of *HOX*-induced transformations may occur independently of *Meis* or involve other factors able to replace *Meis* function.

To investigate the leukemogenic activity of *NUP98-HOXA9*, we generated transgenic mice in which the *NUP98-HOXA9* fusion gene was specifically expressed in the myeloid lineage under the control of the cathepsin G promoter. Approximately 20% of the transgenic (Tg) mice developed AML after long latency periods, which indicated that additional cofactors were required for complete leukemogenesis.

After crossing the Tg mice onto the BXH2 strain, we used retroviral insertional mutagenesis to identify novel cofactors for *NUP98-HOXA9* in addition to *Meis1*. Cooperation between *NUP98-HOXA9* and novel cofactors were then confirmed in a transformation assay using NIH 3T3 cells. Our study provides a model for the application of retroviral insertional mutagenesis to the discovery of cooperative oncogenes.

Materials and methods

Generation of *NUP98-HOXA9* transgenic mice

To generate the *NUP98-HOXA9* transgene, the entire coding sequence of the chimeric *NUP98-HOXA9*¹⁰ was amplified by reverse transcriptase-polymerase chain reaction (RT-PCR) and inserted into the human cathepsin G gene cassette.²³ The purified construct was microinjected into (C57BL/6J × DBA/2J)F₂ fertilized eggs, and transgenic founders were identified by Southern blot hybridization as previously described.²⁴

NUP98-HOXA9 Tg mice (line 1589) were backcrossed to BXH2 mice over 3 generations to introduce the transgene into the BXH2 genetic background, and the leukemia-free survival rates were compared between Tg-positive and Tg-negative BXH2 mice at the third generation of the cross. Mice were monitored daily for evidence of disease, and smear samples of peripheral blood were examined every month. The survival rate of each group was evaluated using the Kaplan-Meier test.

RNA extraction and RT-PCR

Total RNA was extracted from mouse and Sca-1-enriched bone marrow (BM) cells tissues using RNAzol (TelTest, Friendswood, TX). RT-PCR was performed as previously described.¹⁰ The PCR primers used for RT-PCR were as follows: *Fusg2*, 5'-AAAGTTGAGGGGGGGCATTAG-3'; *Cggt2*, 5'-TCATTCTGGATGGTCCGCTG-3'; *Dnal4* forward, 5'-GGAGAGACT-GAAGGGAAGAAAGA-3'; *Dnal4* reverse, 5'-TTGCAGCACTCTC-ATTGTTG-3'; *Fcgr2b* forward, 5'-CAGGTGCTCAAGGAAGACAC-3'; *Fcgr2b* reverse, 5'-TCCCATTCCCTGTGATCAG-3'; *Fcrl* forward, 5'-TCAGCGTGTCTATGACTGG-3'; *Fcrl* reverse, 5'-GTTTCTGAA-GAGCCTGTACCCA-3'; *Con1* forward, 5'-CTCAAGGCACCTTG-CAAGTC-3'; *Con1* reverse, 5'-GTTCCCATCCTGAAAGTCCA-3'; *Con2* forward, 5'-ACGTCACCTCCCGAGAGTCT-3'; and *Con2* reverse, 5'-TAGTCGGAGAGGTGCCTCAG-3'.

Histology and fluorescence-activated cell sorting (FACS)

Tissues were fixed in 10% buffered formalin embedded in paraffin, and sections were stained with hematoxylin and eosin using standard methodologies. For flow cytometry, single-cell suspensions of 1×10^5 cells were incubated with fluorescein isothiocyanate (FITC)-conjugated antibodies, Gr-1 (RB6-8C5), Mac-1 (M1/70), B220 (RA3-6B2), or CD3 (145-2C11) (PharMingen, San Diego, CA) for 20 minutes on ice. Cells were then washed 3 times in $1 \times$ phosphate-buffered saline (PBS) containing 0.1% bovine serum albumin and applied to a FACS-calibur flow cytometer (Becton Dickinson, Mountain View, CA).

Replating assay of bone marrow cells and G-CSF stimulation

Bone marrow was flushed from the femurs of Tg and wild-type mice. Bone marrow cells were washed in PBS, and 1×10^4 cells were plated onto 35-mm Petri dishes in Methocult M3434 methylcellulose medium (Stem Cell Technologies, Vancouver, BC, Canada) supplemented with cytokines (10 ng/mL recombinant mouse [rm] interleukin-3 [IL-3], 10 ng/mL recombinant human [rh] IL-6, 50 ng/mL rm stem cell factor, and 3 U/mL rh erythropoietin). Cultures were incubated at 37°C in a 5% CO₂ humidified atmosphere, and colonies were enumerated after 7 to 11 days. Colonies were then harvested, and 1×10^4 cells were replated in the same way.

For granulocyte colony-stimulating factor (G-CSF) stimulation, Tg and wild-type mice were injected intraperitoneally with 200 μg/kg/d rh G-CSF (Kirin, Tokyo, Japan) for 5 days. White blood cells (WBCs) were counted with Turk solution (MERCK, Darmstadt, Germany), and peripheral blood progenitor cells (PBPCs) were enumerated as the number of colonies formed after 7 days in cultures of 20 μL blood in Methocult methylcellulose medium as described in the preceding paragraph.

Cloning of retroviral integration sites

The cloning of viral integration sites from tumor DNA is described elsewhere.³ Briefly, *NUP98-HOXA9/BXH2* tumor DNA samples were digested completely with *SacII* or *BamHI*, self-ligated, and subjected to nested inverse PCR (IPCR). PCR conditions were 10 cycles of 94°C for 15 seconds, 63°C for 30 seconds, and 68°C for 15 minutes, followed by 23 cycles of 94°C for 15 seconds, 63°C for 30 seconds, and 72°C for 15 minutes with a 20-second extension per cycle. PCR products were analyzed by agarose gel electrophoresis, and tumor-specific products were subcloned and sequenced.

DNA extraction and Southern blot analysis

High-molecular-weight genomic DNA was extracted from frozen leukemic cell suspensions. Samples consisting of 5 μg genomic DNA were subjected to restriction endonuclease digestion, agarose gel electrophoresis, Southern blot transfer, and hybridization as described previously.²⁵ Appropriate genomic DNA fragments derived from flanking sequences of each common integration sites were used as probes.

DNA sequencing and sequence comparison

DNA sequencing was performed using T7 and SP6 primers, integrated DNA, and the Dye Terminator Cyclesequencing Kit (Beckman Coulter, Fullerton, CA). Sequencing reactions were analyzed using a CEQ8000 DNA sequencer (Beckman Coulter).

We compared retroviral integration site sequences with GenBank and UCSC (University of California at Santa Cruz) databases by BLAST (basic local alignment search tool) analysis and located genes in the vicinity of viral integrations for further analysis.

Preparation of a Sca-1-enriched BM cell population by positive selection

Sca-1-enriched BM cells from nonleukemic transgenic and wild-type mice were purified on magnetic cell sorting (MACS) columns using microbead-conjugated Sca-1 antibody. Separation was performed according to the manufacturer's recommendations (MidiMACS; Miltenyi Biotec, Bergisch-Gladbach, Germany).

Retroviral constructs

Retroviral constructs encoding *NUP98-HOXA9* and *Meis1* were described previously.^{19,26} Hemagglutinin (HA) epitope-tagged constructs of the candidate cooperative genes were engineered by fusing the PCR products of each gene in-frame to the 3' end of the HA epitope in the pcDNA3.1 vector (Invitrogen, Carlsbad, CA). The HA-tagged constructs were subcloned into the polylinker of the murine stem cell proviral vector, murine stem cell virus–phosphoglycerate kinase–puromycin resistance gene (MSCV-pgk-puro), as shown in Figure 7A. MSCV-pgk-puro without insert was used as a vector control.

Retroviral stocks and infection of NIH 3T3 cells

Retroviral supernatants were produced as previously described using the plat E packaging cell line (a kind gift from Dr Toshio Kitamura, University of Tokyo).²⁷ Briefly, plasmid DNA was transfected by lipofectamine 2000 (Invitrogen) into plat E cells, and virus-containing supernatants were collected 48 hours after transfection. For infection, 1×10^5 NIH 3T3 cells were plated in 10-cm dishes and were cultured for 24 hours with virus-containing supernatants ($\sim 5 \times 10^5$ colony-forming unit [CFU]/mL as assessed by G-418 or puromycin resistance in NIH 3T3 cells) in the presence of 8 μ g/mL Polybrene (Sigma, St Louis, MO). Cells were then washed with PBS, incubated for 24 hours with Dulbecco modified Eagle medium (DMEM) supplemented with 10% calf serum, and exposed to selection for 10 days in medium containing 1 mg/mL G-418 (GIBCO, Burlington, ON, Canada), and/or 10 μ g/mL puromycin (Sigma) according to the selectable marker in each construct.

Transformation assay

To determine the ability of candidate genes to confer anchorage independent growth, colony formation in soft agar was assessed. Stably transduced cells were seeded at 10^4 cells per dish in 0.3% Agar Noble (Difco, Detroit, MI) over a 0.6% agar bottom layer. After 3 weeks colonies consisting of greater than 50 cells were counted microscopically. The experiment was repeated 3 times, and mean values with standard deviations were calculated.

Western blot analysis

Expression of the retroviral constructs was verified by Western blot analysis. Transiently expressed plat-E cells were lysed in sodium dodecyl sulfate (SDS) sample buffer containing 50 mM tris(hydroxymethyl)aminomethane (Tris) HCl (pH 6.8), 2% SDS, 10% glycerol, 100 mM dithiothreitol (DTT), and 0.1% bromophenol blue, and proteins were separated by SDS–polyacrylamide gel electrophoresis (SDS-PAGE). Size-fractionated proteins were blotted onto polyvinylidene difluoride membranes (Immobilon-P, Bedford, MA). Membranes were blocked in Tris-buffered saline (pH 7.5) with 0.1% Tween-20 (TBS-T) containing 5% skim milk for 1 hour at room temperature and then incubated with monoclonal anti-HA (Roche, Mannheim, Germany), anti-CD16/32 (2.4G2) (for Fc γ 2b; PharMingen), polyclonal anti-Meis1 (kindly provided by Michael Cleary, Stanford University) or anti-HOXA9 antibodies.²⁶ After 3 washes with TBS-T, bound antibodies were detected with horseradish peroxidase–conjugated anti-rat antibody and enhanced chemiluminescence (ECL) Western blotting detection reagents (Amersham, Buckinghamshire, United Kingdom).

Results

Generation of *NUP98-HOXA9* transgenic mice

To determine whether overexpression of *NUP98-HOXA9* induced leukemia, we constructed a transgene containing *NUP98-HOXA9* cDNA under the control of sequences that regulate the promyelocyte-specific expression of the human Cathepsin G (*hCG*) gene (Figure 1A).²³ Five independent founder lines were generated, and bone marrow–specific expression of the transgene was confirmed in all the lines by RT-PCR (Figure 1B). Transgene expression was

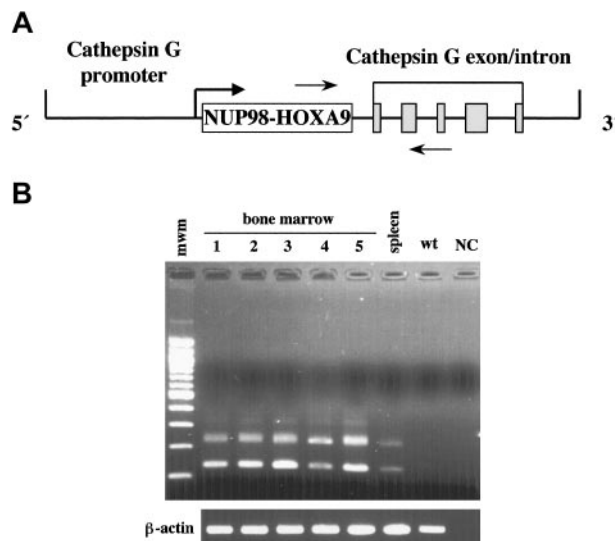


Figure 1. Generation of *NUP98-HOXA9* transgenic mice. (A) The *hCG-NUP98-HOXA9* transgenic construct. The *NUP98-HOXA9* cDNA was inserted at the transcriptional start site of the *hCG* gene. The solid gray boxes represent the 5 exons of the *hCG* gene. The polyadenylation signal is provided by the *hCG* gene. The horizontal arrows indicate the location of RT-PCR primers. (B) RT-PCR analysis of bone marrow RNAs obtained from the transgenic mice of 5 lines (1, line 60; 2, line 131; 3, line 1514; 4, line 1583; 5, line 1589) and spleen of line 1589. Lines 131 and 1589 were used for further analysis. Two different kinds of transcripts were created due to alternative splicing of cathepsin G exons. β -actin was amplified from the same samples to check for RNA quality. mwm indicates 100 base pair (bp) ladder; wt, bone marrow of the wild-type mouse; and NC, negative control.

limited to the bone marrow and the spleen at the lower level, with no expression detected in any of the other tissues examined. The *NUP98-HOXA9* protein was not detected in the bone marrow by Western blotting, probably due to low expression level (data not shown). Two of 5 lines (1589 and 131 in Figure 1B) were maintained, and leukemia developed in the subset of mice of both lines. Line 1589 was selected for further analysis, since the leukemia incidence in this line was a little higher than in line 131 (10% versus 7% at 1 year of age).

Development of myeloid leukemia in *NUP98-HOXA9* transgenic mice

Ten percent of the transgenic mice developed chronic myeloproliferation and subsequent AML by 1 year of age, and 22% by 15 months (Figure 2A; Table 1). Diseased mice showed pale bone marrow as well as lymphadenopathy and hepatosplenomegaly. Blood smears from transgenic mice in the myeloproliferative stage showed increased numbers of abnormal myelomonocytic cells (Figure 2B), and at their leukemic phase more than 20% blasts were shown in bone marrow (Figure 2C). Histologic examination of diseased animals revealed that the normal hematopoietic system in the bone marrow was completely replaced by blastic cells, and that these blastic cells had infiltrated to the lymph nodes, spleen, and liver (Figure 2D). Leukemia of each mice could be classified into myeloid leukemia with or without maturation, myelomonocytic leukemia, or megakaryocytic leukemia, according to the classification of the Bethesda proposals (Figure 2E-G).²⁸

FACS analysis of bone marrow and spleen cells was performed to examine cell-surface antigen expression. Samples from transgenic leukemic mice showed a markedly increased population of cells positive for Gr-1 and Mac-1 antigens (Figure 2H), which clearly indicated a leukemia of granulocytic origin. This myeloid

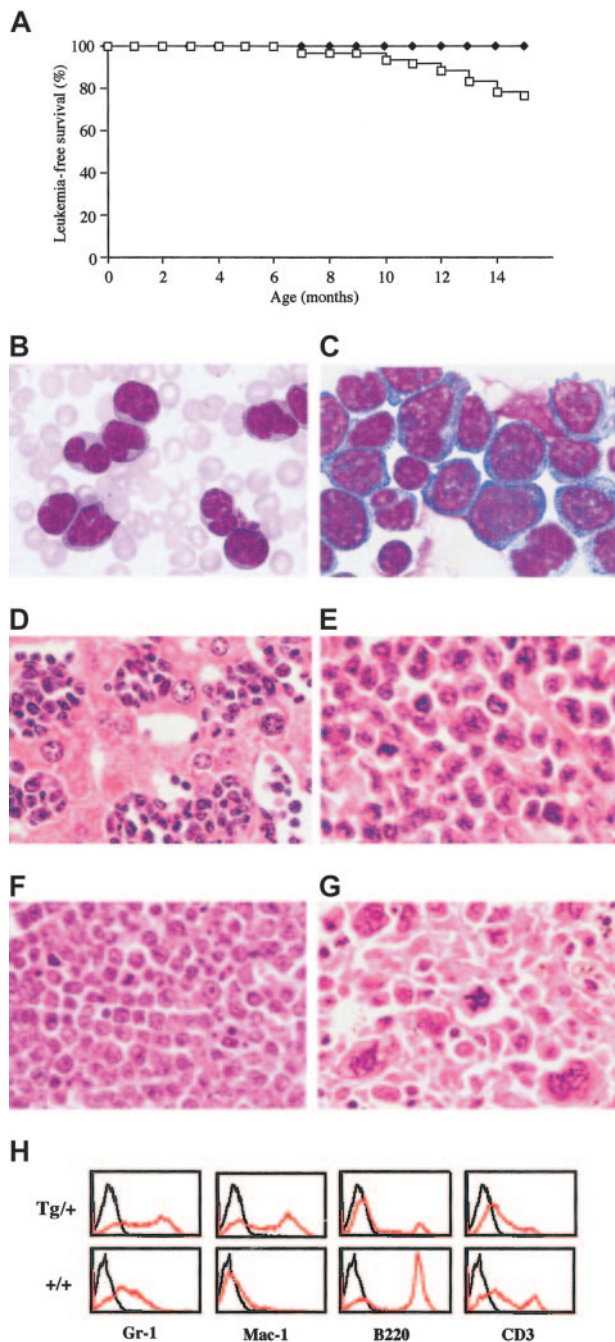


Figure 2. Development and characteristics of leukemias in the Tg mice. (A) Leukemia-free survival curve of the Tg mice. (B) Wright-Giemsa–stained smear of peripheral blood showing leukemia cells displaying abnormal myelomonocytic morphology with immature nuclear segmentation at the myeloproliferative stage (magnification, $\times 1000$). Images were visualized at indicated original magnification using an Olympus BX40 microscope equipped with a $40\times/0.75$ or a $100\times/1.30$ objective lens (Olympus, Tokyo, Japan). Images were photographed with an Olympus C4040 digital camera and acquired with Adobe Photoshop 4.0 J software (Adobe Systems, San Jose, CA). (C) Bone marrow smear of myeloid leukemia with maturation showing many myeloblasts (Wright-Geimsa; magnification, $\times 1000$). (D) Histologic analysis showing leukemic blasts infiltrating in the liver (hematoxylin and eosin [H&E]; magnification, $\times 200$). (E) Myeloid leukemia with maturation (H&E; magnification, $\times 400$). (F) Myeloid leukemia without maturation (H&E; magnification, $\times 400$). (G) Megakaryocytic leukemia (H&E; magnification, $\times 400$). (H) Flow cytometric analysis of leukemic Tg spleen cells compared with wild-type littermates. Cells in suspension were stained with Gr-1, Mac-1, B220, and 2C11 antibodies conjugated with fluorescein isothiocyanate and depicted by the solid lines.

lineage expansion was not observed in wild-type littermates and nonleukemic transgenic mice.

Alteration of the proliferative ability of progenitor cells expressing *NUP98-HOXA9*

Given the relatively low incidence of leukemia in the transgenic mice, we examined whether the transgenic bone marrow cells exhibited any abnormal growth properties. To evaluate the self-renewal capacity of progenitor cells expressing *NUP98-HOXA9*, we performed replating assays using bone marrow cells derived from nonleukemic transgenic mice in methylcellulose cultures. Seven to 11 days after plating, entire methylcellulose cultures from *NUP98-HOXA9* transgenic mice and littermate mice were harvested, and 1×10^4 cells were replated in methylcellulose under optimal conditions for the differentiation of multipotential progenitors (see “Materials and methods”). Primary cultures of transgenic bone marrow cells exhibited no difference in terms of number or types of colonies generated as compared with wild-type mice. However, significant differences between transgenic and wild-type littermates were observed on serial replating of the colonies. After 2 to 3 generations in methylcellulose, cultures from wild-type mice no longer formed colonies. In contrast, colonies derived from mice expressing *NUP98-HOXA9* continued to grow and to generate colonies (Figure 3). These results indicated that BM cells from transgenic mice had a significantly higher self-renewal capacity than those from nontransgenic littermates.

We also compared the responses of *NUP98-HOXA9* transgenic mice and wild-type mice with G-CSF. As shown in Figure 4A-B, after 3 days of G-CSF injections wild-type mice demonstrated marked neutrophilic leukocytosis, with a 30-fold increase in peripheral blood WBC and PBPC numbers. WBCs and PBPCs derived from the transgenic mice showed even higher increases, 2.9-fold and 2.8-fold compared with wild-type, respectively, on day 3. These results clearly indicated that *NUP98-HOXA9* expression induced G-CSF hypersensitivity.

Taken together, these results demonstrate that expression of *NUP98-HOXA9* significantly enhances the proliferative potential of myeloid progenitors. As a result, *NUP98-HOXA9*–expressing bone marrow cells might obtain a sufficient window of time to obtain sequential genetic alterations, so that they could acquire even more growth advantages.

NUP98-HOXA9 accelerates BXH2 myeloid disease

To identify cooperative genes for *NUP98-HOXA9* in leukemogenesis, we transferred the *NUP98-HOXA9* transgene into the BXH2 genetic background for 3 generations by backcross mating. BXH2 mice offer a valuable model system for identifying cooperative genes, as virtually 100% of BXH2 mice develop acute myeloid leukemia by 1 year of age.^{25,29} The high incidence of leukemia in BXH2 mice is causally associated with the expression of a horizontally transmitted B-ecotropic murine leukemia virus. Ecotropic viruses induce disease by insertional activation of proto-oncogenes or insertional inactivation of tumor suppressor genes.³⁰ Genes that cause leukemia in BXH2 mice have already been systematically identified using a proviral tagging technique.^{3,4}

The incidence and latency of myeloid leukemias in *NUP98-HOXA9*/BXH2, wild-type BXH2 and C57BL/6J background *NUP98-HOXA9* transgenic mice were compared. As shown in Figure 5, *NUP98-HOXA9*/BXH2 mice developed acute myeloid leukemia faster than BXH2 and transgenic mice at the time point

Table 1. Characteristics of diseased *NUP98-HOXA9* transgenic mice

Mouse ID	Sex	Time of leukemia onset, d	Organs with leukemic cell invasion	Diagnosis	% blast in BM
1688	F	471	BM, LN, Sp, Th, Lv, Lu, P, U	Myeloid leukemia with maturation	37.0
2484	F	303	BM, Sp, Lu	Myelomonocytic leukemia	36.0
2539	F	309	BM, LN, Sp, Th, Lv	Myeloid leukemia without maturation	85.2
10001	F	394	BM, LN, Sp, Th, Lv, Lu, Sa, A, Tr, K, H, GI	Myeloid leukemia with maturation	29.2
10003	M	413	BM, Sp, Lv, Lu, A, Te	Megakaryocytic leukemia	49.8
10005	M	415	BM, LN, Sp, Lv, K	Myeloid leukemia with maturation	40.6
10009	F	196	BM, LN, Sp, Lv, A, K, GI	Myeloid leukemia with maturation	27.0
11010	M	221	BM, LN, Sp, Lv, Lu, K	Myeloid leukemia without maturation	88.1
11011	M	417	BM, LN, Sp, Th, Lv, Lu, Sa, A, K, H, GI	Myeloid leukemia without maturation	84.6
11043	M	401	BM, LN, Sp, Lv, K	Myeloid leukemia with maturation	69.0
11050	F	389	BM, Sp, Lv, A	Myeloid leukemia with maturation	25.8
11061	F	356	BM, LN, Sp, Lv, Lu, Sa	Myeloid leukemia without maturation	92.2
11062	F	344	BM, LN, Sp, Th, Lv, Lu, Sa, U	Myeloid leukemia without maturation	90.6
11075	M	383	BM, LN, Sp, Lv, Sa, A, K, H, GI	Myeloid leukemia with maturation	78.6

BM indicates bone marrow; LN, lymph node; Sp, spleen; Th, thymus; Lv, liver; Lu, lung; P, pancreas; U, uterus; Sa, salivary gland; A, adrenal; Tr, thyroid; K, kidney; H, heart; GI, gastrointestinal tract; Te, testis.

between 4 and 8 months. This result suggested that *NUP98-HOXA9* expression accelerated the progression of BXH2 myeloid leukemia, and that cooperative genes for *NUP98-HOXA9* may be located near common retroviral integration sites.

Identification of *NUP98-HOXA9* cooperative genes

To characterize the retroviral integration sites, to identify nearby cooperative genes, host-virus junction sequences were amplified by inverse PCR using *NUP98-HOXA9/BXH2* leukemia DNAs and retrovirus-specific primers.³ From a panel of 19 tumors, we isolated and sequenced a total of 67 retroviral integration sites. The clonality of retroviral integrations at these loci was confirmed by the Southern blot analysis (Figure 6) to exclude the possibility that these sites are mere minor clones incidentally identified as PCR artifacts. Homology searches of integration site flanking DNA sequences using the BLAST alignment tool established by GenBank and the UCSC genome browser (October 2003; <http://genome.ucsc.edu/cgi-bin/hgGateway>) allowed us to determine the location of the individual integration sites. The data will be deposited on the Mouse Retroviral Tagged Cancer Gene Database (MRTCGD; <http://genome2.ncifcrf.gov/RTCGD/>). Of the 67 integration sites, 49 were unique, and a summary of the 49 candidate genes is given in Table 2. Integration sites in each tumor are shown

in Supplemental Table S1, available on the *Blood* website; see the Supplemental Table link at the top of the online article.

Of these 49 integration site loci, 5 were common and resulted in the identification of 6 candidate genes (Table 3). The MRTCGD search revealed only the *Meis1* gene as a common integration site in wild-type BXH2 leukemia. *Meis1* is a known cofactor for the wild-type *HOXA9* as well as chimeric *NUP98-HOXA9*,^{19,26} and the incidence of integration at the *Meis1* gene in *NUP98-HOXA9/BXH2* leukemia was much higher than that in wild-type BXH2 leukemia. This result confirmed that this experimental system was able to efficiently identify cooperative genes for *NUP98-HOXA9*, such as *Meis1*. Moreover, the result also indicated that acceleration of BXH2 leukemia is caused by *NUP98-HOXA9* expression, not by other modifier genes in the transgenic line.

Of the 4 other common integration sites, *Fcgr2b* and *Fcrl* are located within the immunoglobulin G Fc receptor gene cluster on chromosome 1. Since all viral integrations involving this region were located between *Fcgr2b* and *Fcrl*, either or both of these genes may be involved.

The *Dnal4* gene encodes the dynein light chain 4 that is a component of the dynein motor complex. Dynein complexes are involved in the cytoplasmic transportation machinery and have been reported to interact with important tumor-related gene products, including p53 and β -catenin.^{32,33} More important, studies have shown that other dynein light chain proteins, such as Dlc2 and Dlc8, interact with BH3-only proteins, including Bim and Bmf, and may block apoptotic signals by suppressing Bim/Bmf functions.^{34,35}

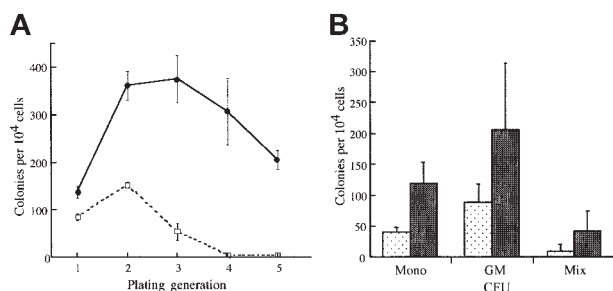


Figure 3. Replating analysis of BM cells derived from Tg mice. (A) Bone marrow was harvested from femurs of Tg mice or wild-type littermate controls, and 1×10^4 cells were plated in culture dishes containing methylcellulose and appropriate medium. Bulk cultures were harvested after 7 to 11 days in culture, and 1×10^4 cells were replated for each sample. Each point represents the number of colonies generated per 1×10^4 cells seeded. Cells (1×10^4) were plated in duplicate dishes, and the mean numbers of colonies for a representative experiment are shown. These data are representative of 5 similar experiments. (B) Classification of colonies in methylcellulose. Colonies at the second replating were analyzed morphologically. Granulocyte-macrophage colony-forming unit (CFU-GM), CFU of monocyte (CFU-mono), and CFU of mixed lineages (CFU-Mix) are increased in the transgenic bone marrow.

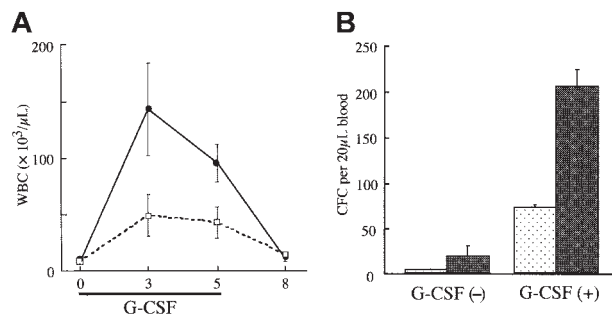


Figure 4. G-CSF hypersensitivity of Tg bone marrow cells. (A) The numbers of white blood cells induced by G-CSF (200 $\mu\text{g}/\text{kg}/\text{d}$ for 5 days) in Tg mice and their wild-type littermate controls. (B) The peripheral blood progenitor cell numbers in Tg mice and their wild-type littermate controls ($n = 2$ for each) after G-CSF injection (200 $\mu\text{g}/\text{kg}/\text{d}$ for 3 days). These data are representative of 3 similar experiments.

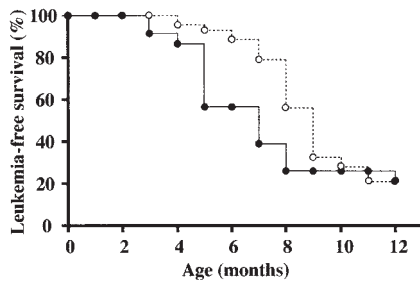


Figure 5. NUP98-HOXA9 accelerates BXH2 myeloid leukemia. Leukemia-free survival rates of BXH2 mice (○) and BXH2/Tg mice (●) were plotted against the age (months after birth). The NUP98-HOXA9 tg mice were backcrossed to the BXH2 strain to introduce the transgene into BXH2 genetic background, and survival rates of Tg-positive BXH2 mice were compared with those of Tg-negative littermates at the third generation.

The *Con1* gene (cooperative gene for NUP98-HOXA9 1) encodes a novel protein that contains an N-terminal short consensus repeat (SCR) domain consisting of 60 amino acid residues. The SCR domain (or Sushi domain) contains 4 cysteines that form 2 disulfide bonds and is thought to be involved in protein-protein interactions. The domain is important for the functional activities of receptor proteins such as soluble IL15R and complement receptors.^{36,37} However, it remains to be clarified what proteins interact with the Con1 SCR domain and how abnormal *Con1* expression promotes NUP98-HOXA9-positive AML.

The *Con2* gene has a C-terminal domain homologous to MurG, a key enzyme in peptidoglycan biosynthesis in bacteria.³⁸ However, its role in mammalian cell systems is unclear.

Expression of candidate cooperative genes in NUP98-HOXA9/BXH2 leukemias

Expression of candidate cooperative genes in NUP98-HOXA9/BXH2 leukemic cells was analyzed by RT-PCR (Figure 7). All leukemic cells with retroviral integrations at each candidate gene

expressed these genes, and leukemias with *Dnalc4*, *Con1*, and *Con2* integrations showed enhanced expression compared with leukemias without integration. *Fcgr2b* was expressed in leukemic cells both with and without integrations, although the former showed slightly enhanced expression. Expression of these 4 genes was very weak in Sca-1-positive normal bone marrow cells. However, the expression level of *Fcrl* was not very different among the leukemia samples. *Fcrl* was also expressed in Sca-1-enriched bone marrow cells, suggesting that *Fcrl* may be expressed in early hematopoietic progenitors. Overall, these observations indicated that most of the candidate cooperative genes are up-regulated by retroviral integration.

Cooperative transforming activity for NIH 3T3 cells

We tested whether the coexpression of NUP98-HOXA9 and each candidate cooperative gene could transform NIH 3T3 cells in soft agar. NIH 3T3 cells were transduced with retroviral vectors bearing individual cooperative candidate genes and colony numbers compared with or without the addition of the NUP98-HOXA9 vector (Figure 8A). Consistent with a previous report,¹⁸ NIH 3T3 cells overexpressing NUP98-HOXA9 alone formed colonies in soft agar more efficiently than control cells (Figure 8C). When *Meis1* was coexpressed with NUP98-HOXA9, transforming activity was significantly enhanced, consistent with the previous finding of cooperative activity in bone marrow cells.²⁶ While NIH 3T3 cells overexpressing *Dnalc4*, *Fcgr2b*, *Fcrl*, and *Con1* alone did not lead to enhanced colony formation, the coexpression of NUP98-HOXA9 led to an additional 2- to 3-fold increase in colony formation compared with NIH 3T3 cells overexpressing NUP98-HOXA9 only. However, coexpression of *Con2* and NUP98-HOXA9 did not enhance the colony-forming ability of NIH 3T3 cells. Thus, *Dnalc4*, *Fcgr2b*, *Fcrl*, and *Con1* cooperatively transformed NIH 3T3 cells with NUP98-HOXA9, such that, while these genes were not transforming genes in the NIH 3T3 assay system in their own

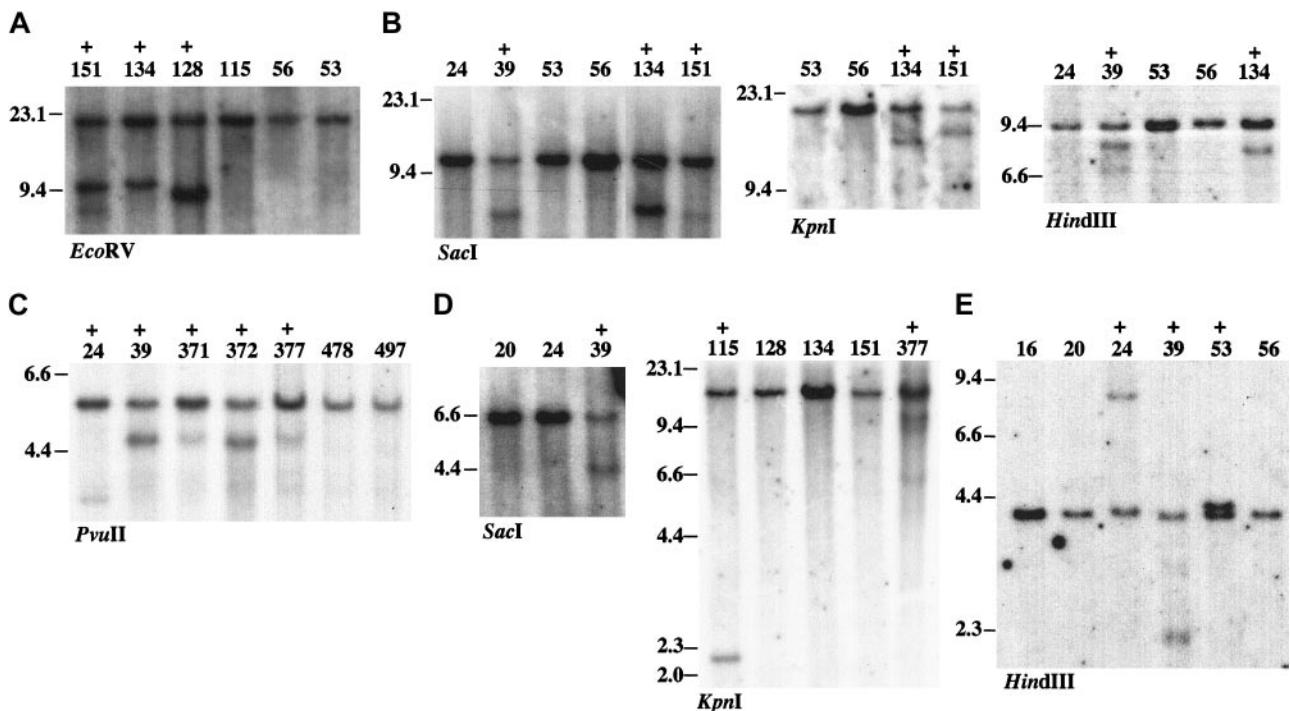


Figure 6. DNA rearrangement at common retroviral integration sites. Southern blot analysis was carried out using 5 μg genomic DNAs extracted from Tg/BXH2 leukemias. The leukemia samples with rearrangements are indicated as + above the sample ID. Restriction enzymes used in each blot are indicated. The size of DNA was indicated in kilobase. (A) *Meis1* using the *Meis1* 3' probe. Tumors with *Meis1* integration at the 3' region show DNA rearrangement. (B) *Dnalc4*. (C) *Fcgr2b/Fcrl*. (D) *Con1*. (E) *Con2*.

Table 2. Retroviral integration sites in *NUP98-HOXA9/BXH2* leukemia

Gene	Protein family	Chromosome location, chromosome No., cM	Tumor ID
Transcription			
<i>Meis1</i>	Homeodomain protein	11, 18.9	14, 15, 16, 53, 128, 134, 151, 478, 497
<i>Sox4</i>	HMG box protein	13, 28.4	151
<i>C/EBPα</i>	bZIP protein	7, 25.6	53
<i>C/EBPϵ</i>	bZIP protein	14, 45.8	15
<i>Ap-4</i>	bHLH-ZIP protein	16, 4.0	24
<i>Myb</i>	Myb transcription factor	10, 21.0	134
<i>Tsga</i>	Testis-specific zinc finger	6, 72.5	371
<i>Mll3</i>	Trithorax homologue	5, 23.8	372
<i>Ncoa6ip</i>	Co-repressor complex protein	4, 3.0	115
Signaling			
<i>Fcgr2b</i>	IgG Fc receptor	1, 172.2	24, 39, 151, 371, 372, 377
<i>Fcrl</i>	IgG Fc receptor	1, 172.2	24, 39, 151, 371, 372, 377
<i>Fcrn</i>	IgG Fc receptor	7, 34.6	478
<i>Snx6</i>	Ser-Thr kinase	12, 49.1	377
<i>Pdgfrb</i>	Receptor tyrosine kinase	18, 61.3	134
<i>Gnas</i>	G protein	2, 175.5	39
<i>Gng3</i>	G protein	19, 8.2	128
<i>Itpr1</i>	Inositol-triphosphate receptor	6, 109.2	371
<i>Aps</i>	Substrate for insulin receptor	5, 134.8	115
<i>Agtrp</i>	Angiotensin II receptor, type 1	4, 143.4	478
<i>Cav2</i>	Caveolin 2	6, 17.1	497
<i>Fdft1</i>	Farnesyl transferase	14, 54.2	56
<i>Rin3</i>	Ras and Rab interacting protein	12, 96.5	16
Metabolism			
<i>XM138092</i>	Mitochondrial ATP synthase	12, 78.9	128
<i>Moat-b</i>	ABC transporter 4	14, 109.8	371
<i>Srd5a2l</i>	Steroid reductase	5, 75.6	39
<i>Kcnd3</i>	Potassium gate channel	3, 106.1	372
<i>Glu decarboxylase</i>	Glu decarboxylase	10, 99.6	56
Apoptosis			
<i>Bad</i>	Pro-apoptotic molecule	19, 3.1	377
Cytoskeleton/membrane traffic			
<i>Dnalc4</i>	Dynein motor complex	15, 80.5	39, 128, 134, 151
<i>Dctn3</i>	Activator of dynein	4, 41.4	377
<i>Transitin</i>	Cytoskeletal protein	7, 53.5	377
<i>Transgelin2</i>	Muscle contractile protein	1, 173.8	134
<i>Pex16</i>	Peroxisomal protein	2, 93.3	371
<i>Tuba2</i>	α -tubulin 2	15, 99.8	16
<i>Prefoldin subunit 6</i>	Microtubule-associated chaperonin	13, 51.3	39
<i>Tspan2</i>	Tetraspanin 2	3, 102.8	375
<i>Zinc transporter 5</i>	15 transmembrane protein	13, 98.2	128
Miscellaneous			
<i>Tgfb1</i>	TGF- β -induced gene	13, 56.1	377
<i>MN1</i>	Fused to TEL in AML	5, 109.1	372
<i>Osa1</i>	Chromatin remodeling complex	4, 131.2	151
<i>Rrm1</i>	Ribonucleotide reductase	7, 92.2	128
<i>Mms2</i>	Ubiquitin conjugating enzyme	15, 31.6	56
<i>Cyclophilin 18</i>	Peptidyl-prolyl <i>cis-trans</i> isomerase	3, 134.8	128
<i>Rpl44</i>	Ribosomal protein L44	12, 63.8	478
<i>Agrip</i>	Agouti-related	8, 105.4	478
<i>Ptma</i>	Prothymosin α	1, 86.9	478
<i>Mrvil</i>	Jaw1 homologue	7, 100.5	371
Unknown			
<i>BI526426 (Con1)</i>	Not determined	13, 48.9	39, 115, 377
<i>AI854024 (Con2)</i>	Not determined	3, 121.7	24, 39, 53

right, the genes cooperated with *NUP98-HOXA9* to promote oncogenesis.

Discussion

Chromosomal translocation with the formation of a chimeric oncogene is a critical and early genetic event in myeloid leukemogen-

esis.^{39,40} In this report, to verify a biologic role for *NUP98-HOXA9* in leukemogenesis, we generated transgenic mice in which chimeric *NUP98-HOXA9* fusion cDNA is specifically expressed in promyelocytes. Approximately 20% of the transgenic mice progresses into AML after a long latent period, although nonleukemic transgenic mice exhibited an increased G-CSF response and a high self-renewal capacity of myeloid progenitors compared with wild-type mice. In many studies, it has been demonstrated that many

Table 3. Common integration sites and cooperative genes in NUP98-HOXA9/BXH2 leukemia

Chromosome locus, No., cM	Candidate gene	Distance from integrations	Incidence in Tg/BXH2, % (n = 19)	Incidence in BXH2, %*
11, 18.9	<i>Meis1</i>	Intragenic 3' or 1 kb upstream	47.4	15
15, 80.5	<i>Dnalc4</i>	Downstream 6-10 kb	21.1	None
13, 48.9	<i>Con1 (B1526426)</i>	Intron 1	15.8	None
1, 172.2	<i>Fcgr2b, Fcrl</i>	Downstream 10-15 kb (<i>Fcgr2b</i>), upstream 15-20 kb (<i>Fcrl</i>)	31.6	None
3, 121.7	<i>Con2 (A1854024)</i>	Intron 1	15.8	None

* The incidence of integration in wild-type BXH2 was described previously (Moskow et al³¹ and Mouse Retroviral Tagged Cancer Gene Database (MRTCGD); <http://genome2.ncicfcrf.gov/RTCGD/>).

other fusion genes are not sufficient to induce leukemia.⁸ Our transgenic model fits well into this natural history of leukemia following translocation, and some cofactors seem to be needed for complete leukemogenesis. We identified novel genes that cooperate with NUP98-HOXA9 for leukemogenesis using retroviral insertional mutagenesis.

It is interesting to speculate as to how these newly cooperative genes promote leukemogenesis. In BXH2 mouse leukemias, 90% of cases with viral integration at *Hoxa7* or *Hoxa9* showed cooperative activation of *Meis1*.²⁰ In other studies, both wild-type *Hoxa9* and chimeric NUP98-HOXA9 were able to cooperate with *Meis1* in myeloid leukemogenesis.^{19,26} However, in our study, only half of the leukemias showed cooperation between NUP98-HOXA9 and *Meis1*. This suggested that some of the cooperative genes identified in this study may have replaced the leukemogenic function of *Meis1*. An example of this might be *Con1*, as *Con1* integration sites never overlapped with *Meis1* integration sites in a single tumor. In contrast, leukemias exhibiting *Meis1* integration also showed integration at the *Dnalc4* locus (Table 2), which suggested that the 2 genes functioned in different leukemogenic pathways. Like other dynein light chain proteins, it is very likely that *Dnalc4* binds to proapoptotic proteins such as Bim and Bmf. Our preliminary experiments showed interaction in vivo between *Dnalc4* and the extra-long isoform of Bim protein (Daisuke Takahashi and T.N., unpublished data, September 2004). In this case, overexpression of *Dnalc4* may block Bim function to give an antiapoptotic potential to preleukemic cells.⁴¹ This hypothesis is supported at least in part by the findings in a previous study that *Meis1* did not enhance the antiapoptotic activity of myeloid cells. Moreover, we also identified *Dctn3*, encoding dynactin 3 as a single integration site in this study. Since dynactin is an upstream regulator of dynein,^{42,43} our findings strongly suggested the importance of the Dynein/Dynactin pathway in NUP98-HOXA9 leukemogenesis.

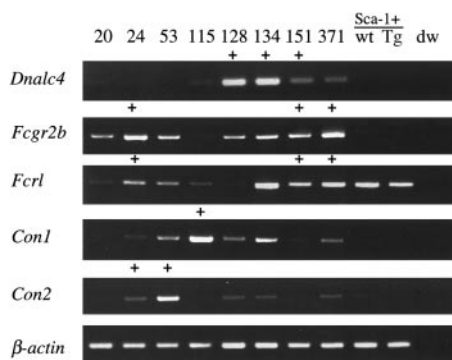


Figure 7. Expression of candidate cooperative genes in NUP98-HOXA9/BXH2 leukemias. RT-PCR analyses of the cooperative genes as indicated. The leukemia samples with retroviral integrations at each loci are indicated as +. Gene expression in Sca-1-enriched bone marrow cells derived from nonleukemic transgenic mice and wild-type littermates were also shown. dw indicates negative control.

Interestingly, *Fcgr2b* is a target for the 1q21 translocation in human follicular lymphoma.^{44,45} While the functional significance of *Fcgr2b* up-regulation remains to be clarified, overexpression of *Fcgr2b* has been reported to enhance nonlymphoid cancer cell

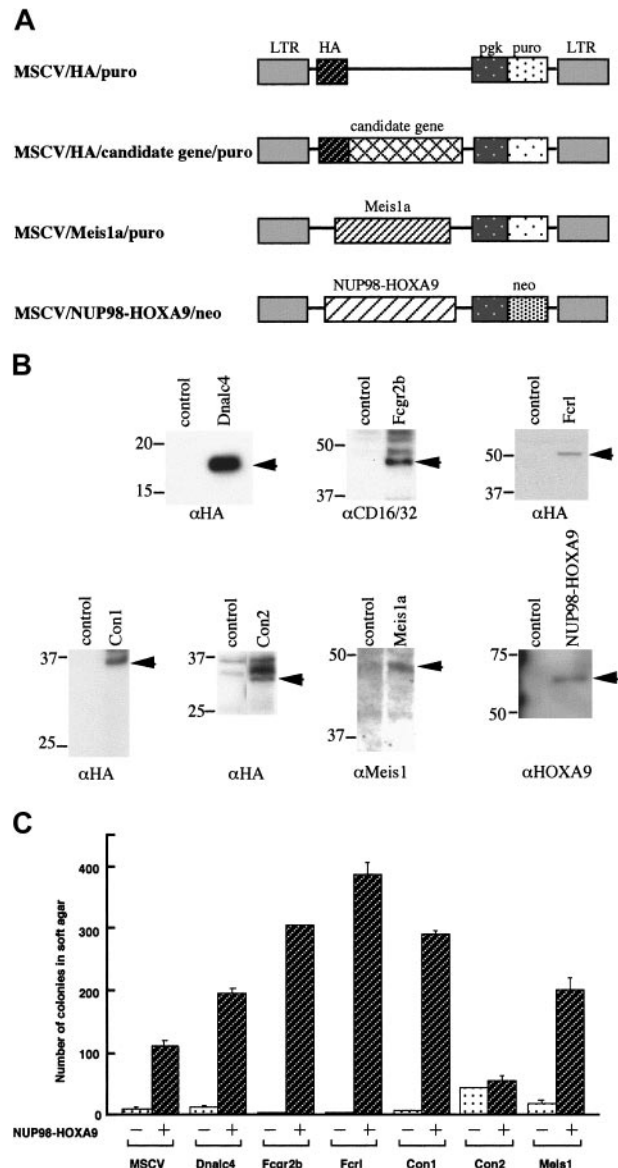


Figure 8. Anchorage-independent growth of NIH 3T3 cells coexpressing NUP98-HOXA9 and cooperative genes. (A) Structure of retroviral constructs for NUP98-HOXA9 and cooperative genes. (B) Western blot analysis. Arrows indicate exogenously expressed proteins detected with the antibodies indicated at the bottom of each panel. (C) The numbers of colonies per 1×10^4 cells seeded were determined 3 weeks after plating in soft agar. Values are the means with standard deviations of 3 experiments. Infected retroviral vectors are indicated at the bottom. Open bars and hatched bars indicate presence of the empty MSCV vector (-) or NUP98-HOXA9 retrovirus (+), respectively.

growth both in vitro and in vivo.^{46,47} As a possibility, it has been demonstrated that Fcγr2b protein seems to be a potent regulator of antibody-dependent cell-mediated cytotoxicity in vivo.⁴⁸ Thus, dysregulation of *Fcγr2b* may play an important role in tumor progression. *Fcrl* is preferentially expressed in germinal center centroblasts and in a subset of diffuse large B-cell lymphoma cells, and the gene has also been reported to serve as a unique marker for the characterization for B-cell malignancy.^{49,50} We also identified another Fc receptor gene, *Fcγr1*, on chromosome 7 as an integration site.⁵¹ Although *Fcγr1* was not a common integration site, our results suggested that signaling pathways involving Fc receptors may be critical for *NUP98-HOXA9*-induced myeloid leukemogenesis.

Studies have demonstrated that *BCR-ABL* cooperates with *NUP98-HOXA9* to cause chronic myeloid leukemia (CML) blast crisis in a mouse model.^{52,53} However, cooperation between 2 different chimeras is practically very rare in human leukemia. In addition, since there is a circumstance where *NUP98-HOXA9* has already been expressed in chronic-phase patients, it is not applied to all cases. Therefore, we have attempted to identify some major cooperative genes, such as *FLT3* in human AML,⁵⁴ for *NUP98-HOXA9* in leukemogenesis.

We tested cooperative transforming activity between *NUP98-HOXA9* and the genes identified in retroviral insertional mutagenesis using NIH 3T3 cells. It has been exhibited that *NUP98-HOXA9* alone could transform NIH 3T3 cells,¹⁸ suggesting that

NUP98-HOXA9 might have common activity to transform both hematopoietic cells and nonhematopoietic fibroblasts, and that this is a reliable if not perfect assay system to evaluate oncogene cooperation. Therefore, *Dnalc4*, *Fcγr2b*, *Fcrl*, and *Con1* are the real cooperative genes cooperating with *NUP98-HOXA9* to promote oncogenesis. It might be useful to introduce those genes into bone marrow cells and then repopulate the cells into irradiated hosts to check cooperative transforming activity in vivo. In this case *Con2* that did not cooperatively transform NIH 3T3 with *NUP98-HOXA9* may be found as a cooperative gene in this system.

In conclusion, our strategy of combining retroviral insertional mutagenesis with a mouse tumor model allowed the efficient identification of cooperative genes with the *NUP98-HOXA9* chimera in leukemogenesis. Our approach can be used to isolate second, third, and subsequent genetic events for known oncogenes and will assist in the clarification of the molecular pathways of carcinogenesis.

Acknowledgments

We thank Miki Takuwa, Deborah Swing, and Bryn Eagleson for technical assistance; Jay Grisolan and Timothy Ley for the cathepsin G promoter; Toshio Kitamura for plat E cells; and Michael Cleary for anti-Meis1.

References

- Malumbres M, Barbacid M. To cycle or not to cycle: a critical decision in cancer. *Nat Rev Cancer*. 2001;1:222-231.
- Hahn WC, Counter CM, Lundberg AS, et al. Creation of human tumour cells with defined genetic elements. *Nature*. 1999;400:464-468.
- Li J, Shen H, Himmel KL, et al. Leukaemia disease gene: large-scale cloning and pathway predictions. *Nat Genet*. 1999;23:348-353.
- Suzuki T, Shen H, Akagi K, et al. New genes involved in cancer identified by retroviral tagging. *Nat Genet*. 2002;32:166-174.
- Mikkers H, Berns A. Retroviral insertional mutagenesis: tagging cancer pathways. *Adv Cancer Res*. 2003;88:53-99.
- Lund AH, Turner G, Trubetskoy A, et al. Genome-wide retroviral insertional tagging of genes involved in cancer in *Cdkn2a*-deficient mice. *Nat Genet*. 2002;32:160-165.
- Hwang HC, Martins CP, Bronkhorst Y, Beijersbergen RL, Brooks MW, Weinberg RA. Identification of oncogenes collaborating with *p27^{Kip1}* loss by insertional mutagenesis and high-throughput insertion site analysis. *Proc Natl Acad Sci U S A*. 2002;99:11293-11298.
- Gilliland DG. Molecular genetics of human leukemias: new insights into therapy. *Semin Hematol*. 2002;4(suppl 3):6-11.
- Borrow J, Shearman AM, Stanton VP Jr, et al. The t(7;11)(p15;p15) translocation in acute myeloid leukaemia fuses the genes for nucleoporin *NUP98* and class I homeoprotein *HOXA9*. *Nat Genet*. 1996;12:159-167.
- Nakamura T, Largaespada DA, Lee MP, et al. Fusion of the nucleoporin gene *NUP98* to *HOXA9* by the chromosome translocation t(7;11)(p15;p15) in human myeloid leukaemia. *Nat Genet*. 1996;12:154-158.
- Fujino T, Suzuki A, Ito Y, et al. Single-translocation and double-chimeric transcripts: detection of *NUP98-HOXA9* in myeloid leukemias with *HOXA11* or *HOXA13* breaks of the chromosomal translocation t(7;11)(p15;p15). *Blood*. 2002;99:1428-1433.
- Taketani T, Taki T, Shibuya N, Kikuchi A, Hanada R, Hayashi Y. Novel *NUP98-HOXC11* fusion gene resulted from a chromosomal break within exon 1 of *HOXC11* in acute myeloid leukemia with t(11;12)(p15;q13). *Cancer Res*. 2002;62:4571-4574.
- Panagopoulos I, Isaksson M, Billstrom R, Strombeck B, Mitelman F, Johansson B. Fusion of the *NUP98* gene and the homeobox gene *HOXC13* in acute myeloid leukemia with t(11;12)(p15;q13). *Genes Chromosomes Cancer*. 2003;36:107-112.
- Taketani T, Taki T, Shibuya N, et al. The *HOXD11* gene is fused to the *NUP98* gene in acute myeloid leukemia with t(2;11)(q31;p15). *Cancer Res*. 2002;62:33-37.
- Raza-Egilmaz SZ, Jani-Sait SN, Grossi M, Higgins MJ, Shows TB, Aplan PD. *NUP98-HOXD13* gene fusion in therapy-related acute myelogenous leukemia. *Cancer Res*. 1998;58:4269-4273.
- Nakamura T, Yamazaki Y, Hatano Y, Miura I. *NUP98* is fused to *PMX1* homeobox gene in human acute myelogenous leukemia with chromosome translocation t(1;11)(q23;p15). *Blood*. 1999;94:741-747.
- Lam DH, Aplan PD. *NUP98* gene fusions in hematologic malignancies. *Leukemia*. 2001;15:1689-1695.
- Kasper LH, Brindle PK, Schnabel CA, Pritchard CE, Cleary ML, van Deursen JM. CREB binding protein interacts with nucleoporin-specific FG repeats that activate transcription and mediate *NUP98-HOXA9* oncogenicity. *Mol Cell Biol*. 1999;19:764-776.
- Kroon E, Krosl J, Thorsteinsdottir U, Baban S, Buchberg AM, Sauvageau G. *Hoxa9* transforms primary bone marrow cells through specific collaboration with *Meis1a* but not *Pbx1b*. *EMBO J*. 1998;17:3714-3725.
- Nakamura T, Largaespada DA, Shaughnessy JD, Jenkins NA, Copeland NG. Cooperative activation of *Hoxa* and *Pbx1*-related genes in murine myeloid leukaemias. *Nat Genet*. 1996;12:149-153.
- Thorsteinsdottir U, Kroon E, Jerome L, Blasi F, Sauvageau G. Defining roles for *HOX* and *MEIS1* genes in induction of acute myeloid leukemia. *Mol Cell Biol*. 2001;21:224-234.
- Calvo KR, Sykes DB, Pasillas M, Kamps MP. *Hoxa9* immortalizes a granulocyte-macrophage colony-stimulating factor-dependent promyelocyte capable of biphenotypic differentiation to neutrophils or macrophages, independent of enforced *Meis* expression. *Mol Cell Biol*. 2000;20:3274-3285.
- Grisolano JL, Sclar GM, Ley TJ. Early myeloid cell-specific expression of the human cathepsin G gene in transgenic mice. *Proc Natl Acad Sci U S A*. 1994;91:8989-8993.
- Perry WL, Nakamura T, Swing DA, et al. Coupled site-directed mutagenesis/transgenesis identifies important functional domains of the mouse agouti protein. *Genetics*. 1996;144:255-264.
- Jenkins NA, Copeland NG, Taylor BA, Bedigian HG, Lee BK. Ecotropic murine leukemia virus DNA content of normal and lymphomatous tissues of BXH-2 recombinant mice. *J Virol*. 1982;42:379-388.
- Kroon E, Thorsteinsdottir U, Mayotte N, Nakamura T, Sauvageau G. *NUP98-HOXA9* expression in hemopoietic stem cells induces chronic and acute myeloid leukemias in mice. *EMBO J*. 2001;20:350-361.
- Morita S, Kojima T, Kitamura T. Plat-E: an efficient and stable system for transient packaging of retroviruses. *Gene Ther*. 2000;7:1063-1066.
- Kogan SC, Ward JM, Anver MR, et al. Bethesda proposals for classification of nonlymphoid hematopoietic neoplasm in mice. *Blood*. 2002;100:238-245.
- Copeland NG, Jenkins NA. Myeloid leukemia: disease genes and mouse models. In: Hiai H, Hino O, eds. *Animal Models of Cancer Predisposition Syndromes*. Basel: Karger; 1999:53-63.
- Jonkers J, Berns A. Tumorigenesis by slow-transforming retroviruses—an update. *Biochim Biophys Acta*. 1990;1032:213-235.
- Moskow JJ, Bullrich F, Huebner K, Daar IO, Buchberg AM. *Meis1*, a PBX1-related homeobox gene involved in myeloid leukemia in BXH-2 mice. *Mol Cell Biol*. 1995;15:5434-5443.
- Giannakakou P, Sackett DL, Ward Y, Webster KR, Blagosklonny MV, Fojo T. p53 is associated with cellular microtubules and is transported to the nucleus by dynein. *Nat Cell Biol*. 2000;2:709-711.

33. Ligon LA, Karki S, Tokito M, Holzbaur ELF. Dynein binds to β -catenin and may tether microtubules at adherens junctions. *Nat Cell Biol*. 2001;3:913-917.
34. Puthalakath H, Huang DC, O'Reilly LA, King SM, Strasser A. The proapoptotic activity of the Bcl-2 family member Bim is regulated by interaction with the dynein motor complex. *Mol Cell*. 1999;3:287-296.
35. Puthalakath H, Villounger A, O'Reilly LA, et al. Bmf: a proapoptotic BH3-only protein regulated by interaction with the myosin V actin motor complex activated by anoikis. *Science*. 2001;293:1829-1832.
36. Muta T, Miyata T, Misumi Y, et al. Limulus factor C: an endotoxin-sensitive serine protease zymogen with a mosaic structure of complement-like, epidermal growth factor-like, and lectin-like domains. *J Biol Chem*. 1991;266:6554-6561.
37. Wei Xq, Orchardson M, Gracie JA, et al. The Sushi domain of soluble IL-15 receptor alpha is essential for binding IL-15 and inhibiting inflammatory and allogenic responses in vitro and in vivo. *J Immunol*. 2001;167:277-282.
38. Ha S, Gross B, Walker S. *E. Coli* MurG: a paradigm for a superfamily of glycosyltransferases. *Curr Drug Targets Infect Disord*. 2001;1:201-213.
39. Rabbits TH. Chromosomal translocations in human cancer. *Nature*. 1994;372:143-149.
40. Look AT. Oncogenic transcription factors in the human acute leukemias. *Science*. 1997;278:1059-1064.
41. Fujino T, Yamazaki Y, Largaespada DA, et al. Inhibition of myeloid differentiation by Hoxa9, Hoxb8, and Meis homeobox genes. *Exp Hematol*. 2001;29:856-863.
42. Boylan K, Serr M, Hays T. A molecular genetic analysis of the interaction between the cytoplasmic Dynein intermediate chain and the Glued (Dynactin) complex. *Mol Biol Cell*. 2000;11:3791-3803.
43. King SJ, Schroer TA. Dynactin increases the processivity of the cytoplasmic dynein motor. *Nat Cell Biol*. 2000;2:20-24.
44. Callanan MB, Le Baccon P, Mossuz P, et al. The IgG Fc receptor Fc γ RIIB, is a target for deregulation by chromosomal translocation in malignant lymphoma. *Proc Natl Acad Sci U S A*. 2000;97:309-314.
45. Chen W, Palanisamy N, Schmidt H, et al. Deregulation of FCGR2B expression by 1q21 rearrangements in follicular lymphomas. *Oncogene*. 2001;20:7686-7693.
46. Witz IP, Ran M. FcR may function as a progression factor of nonlymphoid tumors. *Immunol Res*. 1992;11:283-295.
47. Zusman T, Gohar O, Eliassi H, et al. The murine Fc-gamma (Fc gamma) receptor type II B1 is a tumorigenicity-enhancing factor in polyoma-virus transformed 3T3 cells. *Int J Cancer*. 1996;65:221-229.
48. Clynes RA, Towers TL, Presta LG, Ravetch JV. Inhibitory Fc receptors modulate in vivo cytotoxicity against tumor targets. *Nat Med*. 2000;6:443-446.
49. Facchetti F, Cella M, Festa S, Fremont DH, Colonna M. An unusual Fc receptor-related protein expressed in human centroblasts. *Proc Natl Acad Sci U S A*. 2002;99:3776-3781.
50. Dash AB, Williams IR, Kutok JL, et al. A murine model of CML blast crisis induced by cooperation between BCR/ABL and NUP98/HOXA9. *Proc Natl Acad Sci U S A*. 2002;99:7622-7627.
51. Kandil E, Noguchi M, Ishibashi T, et al. Structural and phylogenetic analysis of the MHC class I-like Fc receptor gene. *J Immunol*. 1995;154:5907-5918.
52. Davis RS, Li H, Chen CC, Wang YH, Cooper MD, Burrows PD. Definition of an Fc receptor-related gene (FcRX) expressed in human and mouse B cells. *Int Immunol*. 2002;14:1075-1083.
53. Mayotte N, Roy DC, Yao J, Kroon E, Sauvageau G. Oncogenic interaction between BCR-ABL and NUP98-HOXA9 demonstrated by the use of an in vitro purging culture system. *Blood*. 2002;100:4177-4184.
54. Gilliland DG, Griffin JD. The roles of FLT3 in hematopoiesis and leukemia. *Blood*. 2002;100:1532-1542.